9803-6005-RU-000

# DEVELOPMENT OF A LUMINESCENT CHAMBER FOR SPACE RESEARCH

by

R. F. Doolittle



Prepared for

HEADQUARTERS
NATIONAL AERONAUTICS AND SPACE ADMINISTRATION
WASHINGTON, D.C.

CONTRACT NO. NASw 285

SEPTEMBER 1963

TRW SPACE TECHNOLOGY LABORATORIES
THOMPSON RAMO WOOLDRIDGE INC.

9803-6005-RU-000

30 September 1963

Final Report

# DEVELOPMENT OF A LUMINESCENT CHAMBER FOR SPACE RESEARCH

Prepared for:

Headquarters
National Aeronautics and Space Administration
Washington, D.C.

Contract No. NASw 285


R. F. Doolittle
Prepared by
R.F. Doolittle

Carl D. Graves
Approved by
C.D. Graves
Project Director

SPACE PHYSICS DEPARTMENT
Physical Research Division

TRW Space Technology Laboratories, Inc.
One Space Park
Redondo Beach, California

TABLE OF CONTENTS

LIST OF ILLUSTRATIONS

FINAL TECHNICAL REPORT ON DEVELOPMENT OF A
LUMINESCENT CHAMBER FOR SPACE RESEARCH

NASA CONTRACT NASw 285

## INTRODUCTION

A preliminary flight prototype of a luminescent chamber has been constructed and tested in our laboratory by using minimum ionizing cosmic ray mu-mesons. As described in our proposal No. 0664.00, the luminescent chamber affords a means of obtaining a visual record of the track produced by a charged particle traversing a scintillation crystal. Unlike scintillation counting, a fraction of the fluorescent light produced along the path of a charged particle as it loses energy in a scintillator is optically coupled and focused onto the photocathode of an image intensifier tube. The photoelectrons thus liberated are accelerated within the tube through a potential difference of the order of 10 kilovolts before impinging upon a fluorescent phosphor screen. A one to one spacial correspondence is maintained between the electron's point of departure at the cathode and its arrival at the phosphor. This is accomplished by appropriate electron-optical focusing which in our case is provided by an external axial magnetic field. In practice several such "stages" are built into a single envelope with a corresponding increase in the overall quantum gain. However, an entirely satisfactory tube of this type with more than three stages has not, as far as we know, been built successfully. Unfortunately, three stages of light gain coupled with the kinds of resolution currently available are not quite sufficient to enable one to record, on photographic film, the image of a single photoelectron released from the first photocathode. This, of course, is the ultimate criterion which must be realized in order to have the most sensitive type of instrument.

Another property required of the image intensifier tubes, in order that they be useful in luminescent chamber physics experiments, is their ability to be electronically switched on and off. By keeping the second stage of a three stage tube off, for instance, and then gating this stage on, as determined by external electronic logic, and for a time comparable to the decay time of the first stage phosphor, only those classes of events of interest to a particular experiment are recorded. In addition, a large gain in the signal-to-noise ratio is achieved. It is evident that by selecting a fast decay phosphor for the first stage, that fast time resolution may be accomplished and that in a field of high particle flux it is possible to separate out and record only those events or particles of interest. It is this feature plus the high spacial resolution and post event triggering capability that makes the luminescent chamber an appealing instrument at high energy particle accelerators. For space physics research where, in general, the particle fluxes are relatively small, one can utilize a slower decay phosphor with its intrinsic increase in efficiency.

## THE STL LUMINESCENT CHAMBER FLIGHT INSTRUMENT

In designing and building the flight prototype instrument, the following main categories were considered: 1) image intensifier tube selection; 2) image intensifier tube power supply design; 3) choice of initial space physics experiment; 4) the design of an appropriate track forming scintillator; 5) the design and fabrication of a film camera suitable for balloon experiments; 6) electronics design and fabrication for (a) image intensifier tube gating and camera control and (b) that associated with the first experiment to be performed; 7) overall mechanical design and assembly; and 8) final testing of the completed instrument. These categories will be discussed in order.

## 1. Image Intensifier Tube Selection

As mentioned in the introduction a single three-stage tube of the type described does not, at least of those presently available, provide sufficient photon gain for recording on film the result of a single photoelectron emitted from the first cathode. It should be pointed out that other types of image intensifier tubes are being built on a developmental basis by various companies, that in principle would have sufficient gain. However, this type of tube has only one final output phosphor, and hence no "memory", which makes it unsuitable for post event triggering.

The requirements of high gain and resolution, low voltage gating grids, intermediate phosphor memory, small size, and light weight, led us to select two three-stage magnetically focused tubes developed by RCA. These tubes could be provided with fiber optic faceplates at either the input or output end or both. This feature eliminates the need for external refracting optics for intertube coupling and for coupling from the output phosphor of the second tube to the film camera. In addition, a greater light collection efficiency is realized. RCA originally contracted to supply two such tubes including the appropriate cylindrical magnet required for focusing. The first tube was to have a glass input window and fiber optic output. It was to be supplied with low voltage shutter grids on both the first and second stages, an output resolution of 18 line pairs per millimeter, and P-11 type phosphors throughout. Its quantum gain when coupled with the second tube was to be $6.25 \times 10^8$. The purpose of the first stage shutter grid was to increase the versatility by enabling one to use the instrument in high particle fluxes and relying on the 1/4 microsecond decay time of the NaI track forming chamber itself as the storage mechanism. The second three-stage tube was ordered with specifications the same as the first except that both input and output were to have fiber optic faceplates and only the second stage was to have a gating grid. It was also specified that the two tubes were to be operated electrically in parallel.

In the course of their development RCA encountered a series of technical obstacles which they had not anticipated in attempting to meet these specifications although we had been assured initially that the development would be straightforward. These problems were concerned primarily with the fiber optics, the gating grids, and the permanent magnet, and their final solution resulted in a delivery date 16 months later than originally promised.

The fiber optic problem had to do with obtaining faceplates that would not leak when the tubes were evacuated, that would have sufficient dielectric strength to withstand the 21-24 kilovolts appearing between the first tube output fiber and second tube input fiber, and that had a minimum of optical "cross-talk" between individual fiber elements. The final solution to this problem was realized by RCA's eventually obtaining some vacuum tight fiber bundles but also necessitated electrical operation of the tubes in series to avoid high voltage breakdown across the fibers. Various types of gating grids were tested by RCA but each had its disadvantages. A compromise was eventually reached which appears to be quite satisfactory. Although permanent cylindrical magnets had been supplied for these types of tubes for single tube systems, the fabrication of a magnet long enough to incorporate two tubes led to difficulties in maintaining a uniform axial magnetic field over this distance. This non-uniformity results in a loss of resolution. Our calculations showed that an overall system resolution of about 8 line pairs per millimeter would still be satisfactory and our purchase order was modified accordingly.

A further delay was encountered after receiving the tubes. It was ascertained that some of the celastic potting compound, that had been used by RCA to mount and hold the tubes within the magnet, had flowed between the fiber optic interface coupling between the two tubes. This, of course, resulted in a serious loss of resolution and gain and necessitated a complete disassembly of the tubes from the magnet by us at STL. A special mechanical device was designed and fabricated in order to properly reassemble the tubes and assure good optical coupling between them. The image tube and magnet assembly is now operational and very good track pictures of cosmic ray mu-mesons have been obtained (see Fig. 17).

A schematic representation of the image tube and magnet assembly is shown in Fig. 1 and an actual photograph in Fig. 2.

2. Image Intensifier Tube Power Supply

High voltage, low current, power supplies are necessary to provide the accelerating potentials and the proper electrostatic field for the image intensifier tubes. The voltages required to operate each tube are -21 kv and +24 kv for the first and second tubes respectively. All intermediate tube voltages are obtained from a resistor divider (see Fig. 9). The quiescent D.C. current in the divider is $\sim 10^{-5}$ amperes. An analysis was made of the maximum amount of charge transferred in the tubes during the time an event is being recorded, and capacitors were selected that would insure a maximum voltage drop during this time of less than 0.1%. The duty cycle is such that the charge will be replaced to at least 99% of its initial valve before the next event. The operation design parameters for the power supply were determined and an order for its fabrication was awarded to Grafix, Inc., Albuquerque, New Mexico. The unit is built entirely of solid state components, will operate from a 28 volt battery, and measures 3" x 4" x 5".

3. Choice of Initial Space Physics Experiment

The luminescent chamber system, may be broken down into three main subsystems. First, the image intensifier tube assembly along with its power supply and all of the associated electronics required for generating and applying the appropriate

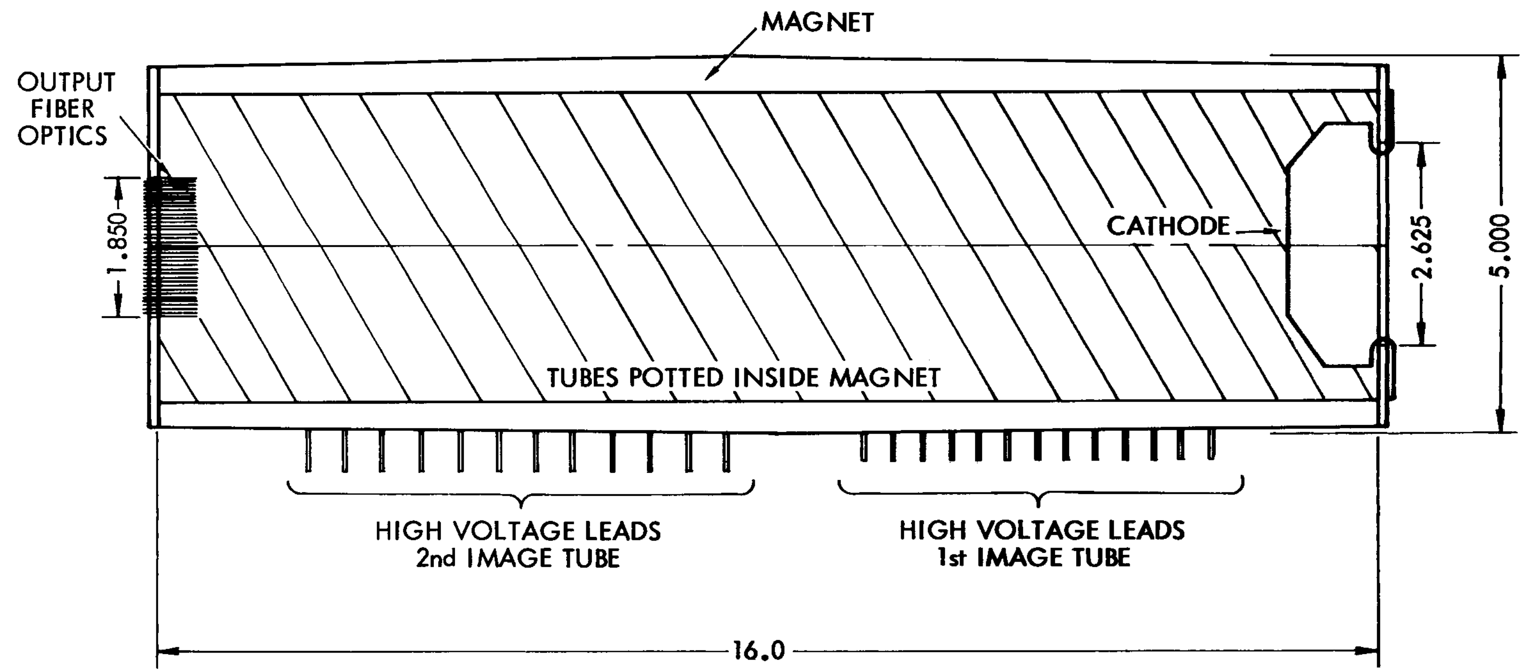


Figure 1. Schematic Diagram of Image Intensifier Tubes and Magnet

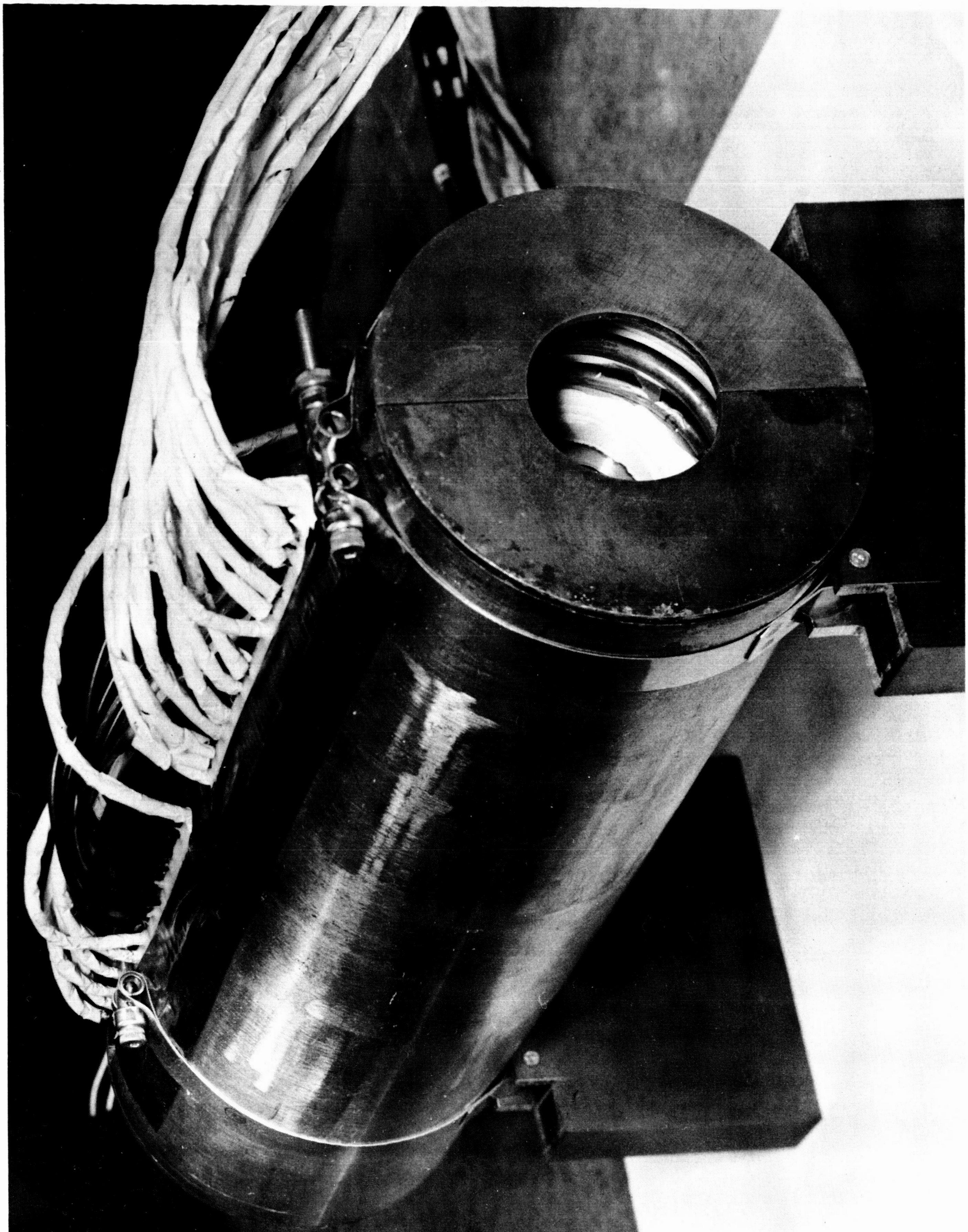

Figure 2. Magnet and Support Assembly Surrounding Image Tubes

gating pulses to the tubes; second, the device used to record the track information appearing at the output phosphor of the image tube assembly which in general would be either a film camera or a television camera; and third, the track forming chamber itself, including appropriate triggering counters and electronics.

The first subsystem (image tube assembly) and to a certain extent the method of recording, is independent of the particular choice of experiment. However, the track forming chamber and triggering mode will, in general, change from experiment to experiment. Therefore, as part of our development of a flight prototype instrument it was necessary to select a particular initial experiment. The choice of an initial experiment was based on the following considerations: a) that the experiment be relatively simple and straightforward, b) that it provide a good test of the luminescent chamber as an important instrument for space physics investigations, c) that the fundamental results of the experiment be easily verified by comparison with data obtained from previous similar measurements, d) that the use of the luminescent chamber in the particular experiment be unique and e) that the results obtained contribute to a better understanding of the phenomena involved.

As a result of these considerations the decision was made to investigate in detail the charge and energy spectra of primary cosmic rays from charge $Z = 2$ through $Z = 8$, i.e., from helium nuclei through oxygen nuclei. The experiment is to be performed in a pressurized gondola carried by a balloon to heights greater than 100,000 feet above sea level. The track picture of each event will be supplemented by pulse height information from counters surrounding the chamber. For each primary nucleus traversing the track forming and counter assembly, the pulse height from an energy loss ($dE/dx$) counter and from a Cerenkov counter is to be recorded along with the track picture. This "simultaneous" pulse height analysis will suffice to resolve the charge of the incident particle. (See Fig. 3.) Since the charged primary

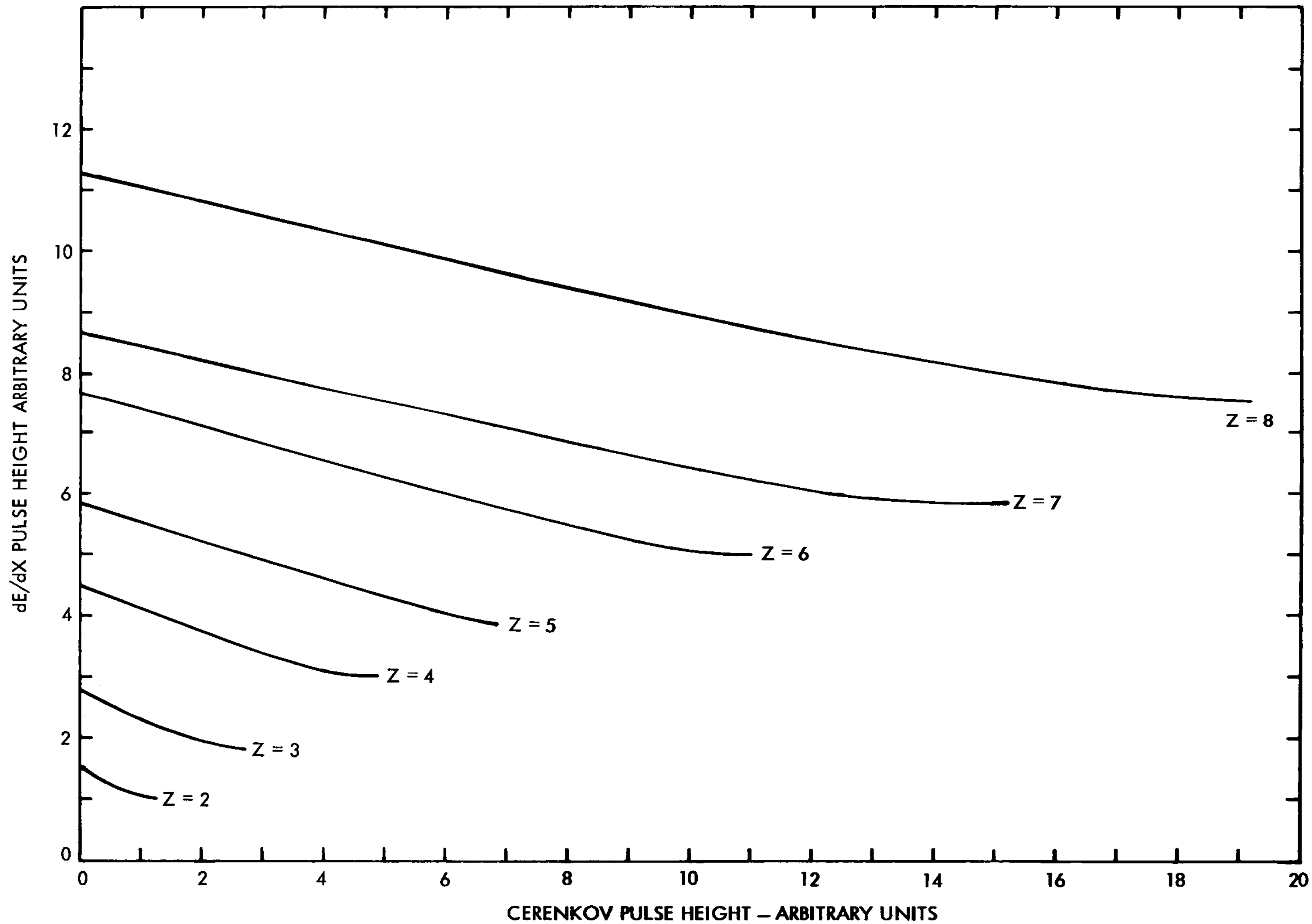


Figure 3. dE/dx vs. Cerenkov Pulse Height as a Function of Charge (Z)

high energy cosmic rays consist of bare nuclei, a measure of the net charge serves to identify the mass as well. Isotopic effects are to be ignored in the present experiment. From a knowledge of the charge, mass, and energy loss it is then a simple matter to calculate the energy. The geometrical arrangement of the counter and track forming assembly is described in more detail in the following section.

## 4. The Track Forming Scintillator and Counter Assembly

It was decided to design the track forming scintillator and associated counters as an integral, hermetically sealed, unit. The reasons for this are described at the end of this section. The configuration of the assembly is shown in Fig. 4. The unit is divided into 5 optically insulated slabs with a sealed glass faceplate on the front surface. Crystals A, C, and E are track forming sections of NaI(Tl) scintillation material. Crystal B is made of ultraviolet transmitting grade lucite. It is packaged in dry contact with $Al_2O_3$ spray on 5 mil foil and serves as the Cerenkov radiator. Crystal D serves as the energy loss detector and is made of NaI(Tl) but with a graded reflector to maximize uniformity of response.

The walls of the track forming sections with the exception of those coupled to the front glass window are polished and painted with RB13 compound and carbon black. This technique minimizes scattered and reflected light in the crystal which could result in unwanted background in the track pictures. Light pipes are brought out of the crystal housing from crystals B and D to be coupled to photomultiplier tubes. The anode pulse height from these tubes is recorded for each event. In addition, a light pipe is also brought out from a side face of crystal A. The dynode pulses from this counter along with the dynode pulses from counters B and D are fed to a three-fold coincidence circuit whose output defines an event. The electronic details are discussed in Section 6b. The counter/track assembly, less the photomultiplier tubes, was fabricated by the Harshaw Chemical Company. It is

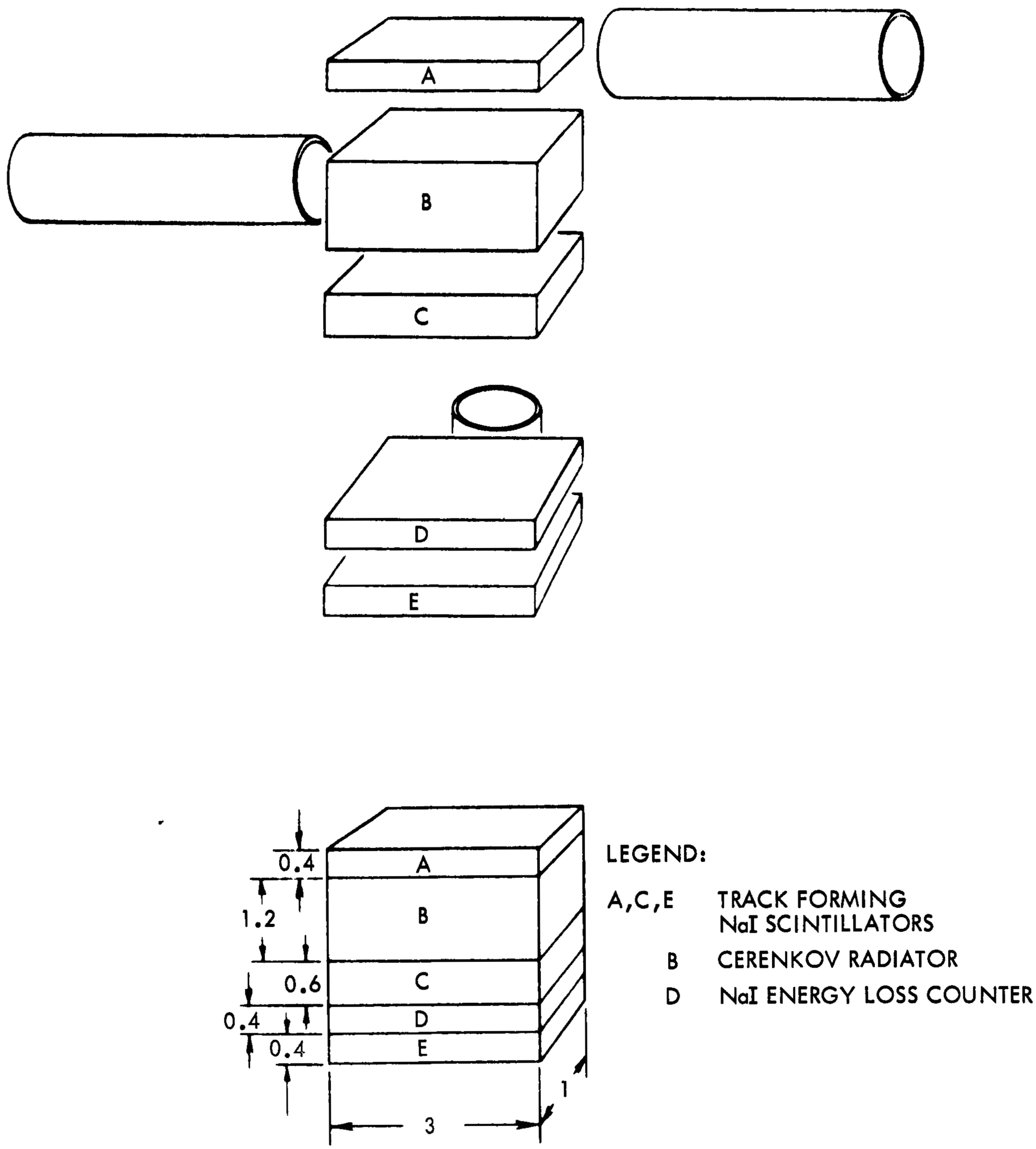


Figure 4. Schematic Drawing of Chamber/Counter Assembly

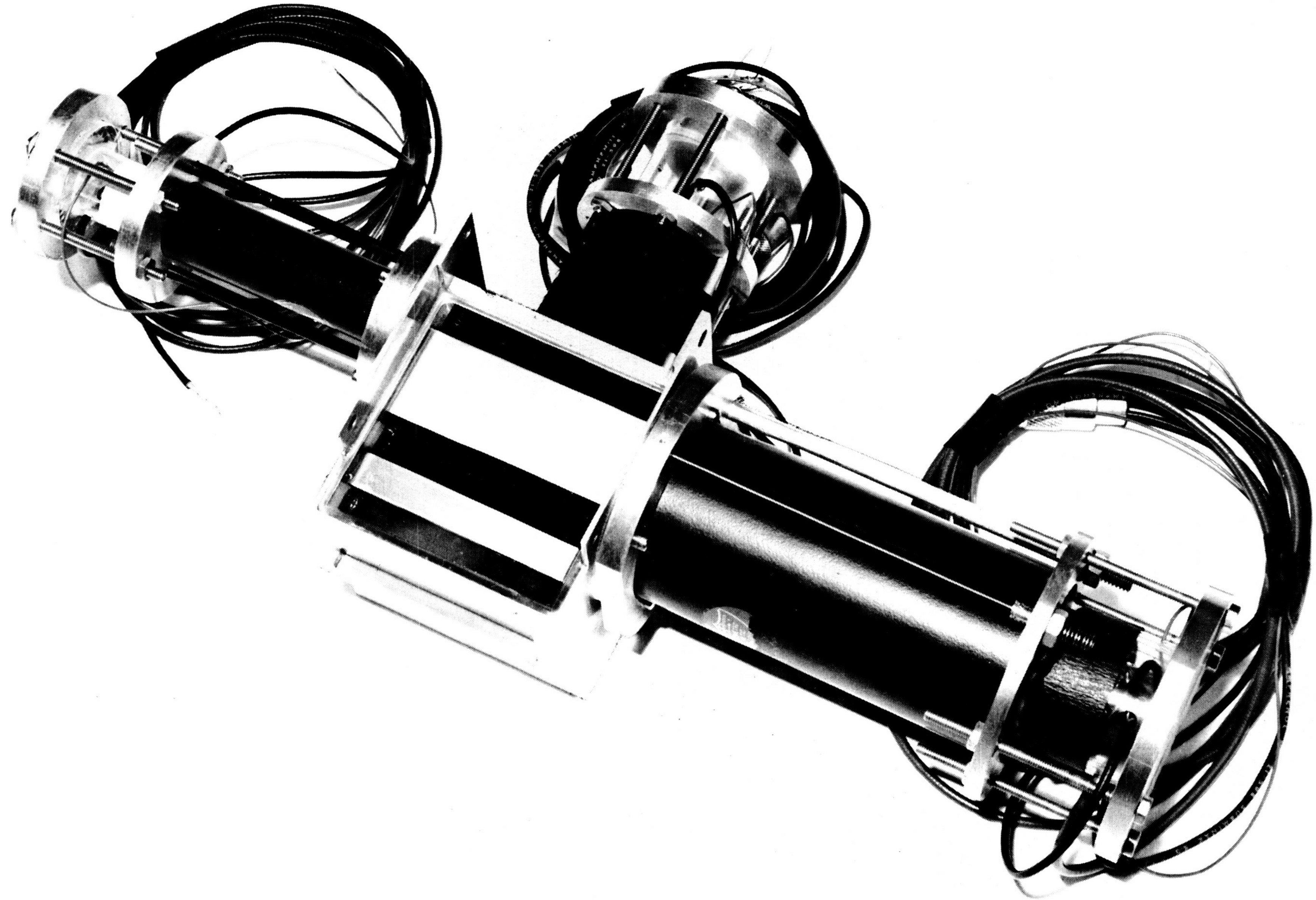

Figure 5. Photograph of Chamber/Counter Assembly Including Photomultiplier Tubes

packaged in a ruggedized aluminum mount filled with $10^6$ centistoke silicon oil. Fig. 5 is a photograph of this assembly including the photomultiplier tubes.

The geometrical arrangement, as described above, enables one to observe the particle before it enters the Cerenkov counter and again as it leaves. Similarly, the same particle is observed prior to entering and after emerging from the dE/dx counter. In this fashion,if the track segments fall on a straight line, it can be stated with a high degree of reliability that no local nuclear interactions have occurred in the counters themselves. Therefore, the pulse heights, as measured, should represent "good" information and the interaction background is eliminated. A schematic representation of an event is shown in Fig. 6. Secondly, each event contains directional information in the track picture. This fact enables one to afford a relatively large solid angle since the path length of the particle through the crystal is known. The pulse height which one measures in such a case is a function of the particles' path length through the medium. It is also expected that ionization density measurements will be possible from the track pictures and results consistent with the pulse height information would further increase the reliability of the experiment. A block diagram of the entire system is presented in Fig. 7 and the electronic details are discussed in Section 6.

## 5. The Design and Fabrication of a Film Camera for Balloon Experiments

There were a number of special considerations that went into the design of the film camera (Fig. 8). It was decided to design the camera to carry 1000 feet of 35 mm roll film. The entire magazine was to be made of non-magnetic parts and be as light as possible. Aluminum was therefore the logical choice for the main body of the magazine with stainless steel used for most moving parts. Since the image tubes have a fiber optic output and exposures are made by having the film in direct optical contact with the fiber bundle, it was necessary to include a mechanism for

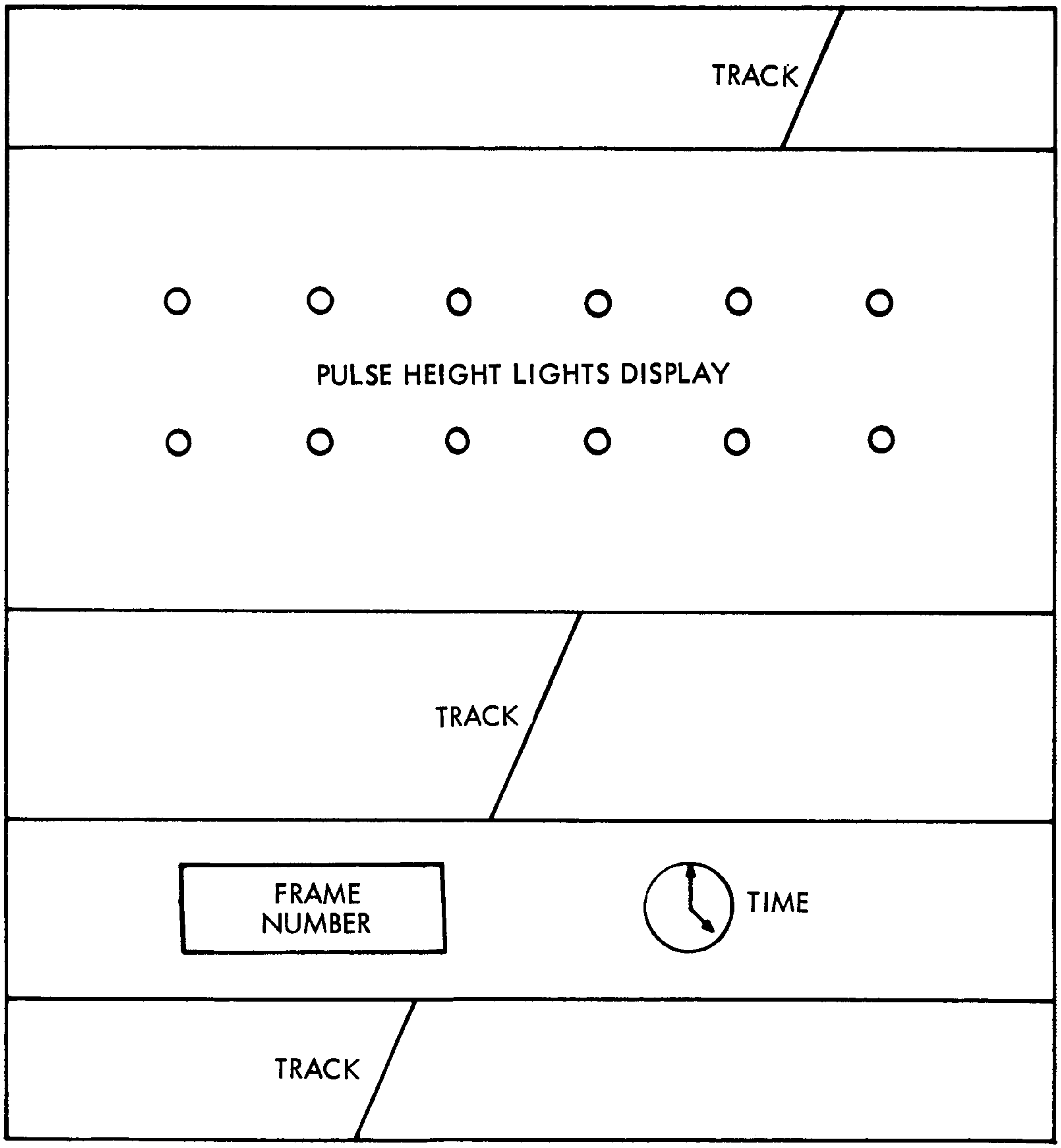


Figure 6. Schematic Representation of an Event on Film

releasing the film from the fiber during each film advance cycle. This was accomplished by a cam arrangement which retracts a longitudinally spring loaded platen prior to advancing the film. The platen is mounted in such a way that, except during the advance cycle, it insures positive seating of the film against the fiber optic. As explained in Section 6b, the two photomultiplier tube anode pulses are fed into two 64 channel pulse height analyzers which in turn drive separate binary scalers. The final state of these scalers for each event is then read out into a sequence of six argon lamps. The appropriate lamps are pulsed on for about 30 milliseconds and recorded as dots on the same film that records the track information. This is accomplished by a special housing on the rear of the platen that accommodates the 12 argon lamps. (See Fig. 8.) The light is piped through 12 small holes to the front of the platen so that the exposure is actually made through the back of the film. The position of the pulse height light display coincides on the film with the position of the Cerenkov counter so that there is no overlap with the track information.

At a different place within the camera, and an integral number of frames from the track and pulse height information, an optical system projects the image of a clock and a frame counter onto the emulsion side of the film. Thus a number is assigned to each event and the time history is also known. This information appears on the film in the same position as the dE/dx counter so that again there is no overlap of information. (See Figs. 6 and 8.)

The time required for the film to advance one frame is from 0.3 of a second to 1 second depending on the camera motor voltage. An electrical interlock, to be described later, inhibits triggering of the entire system until completion of the camera wind cycle. The wind cycle is initiated by an electrical pulse from the coincidence circuit and master pulse logic, after which a cam actuated microswitch

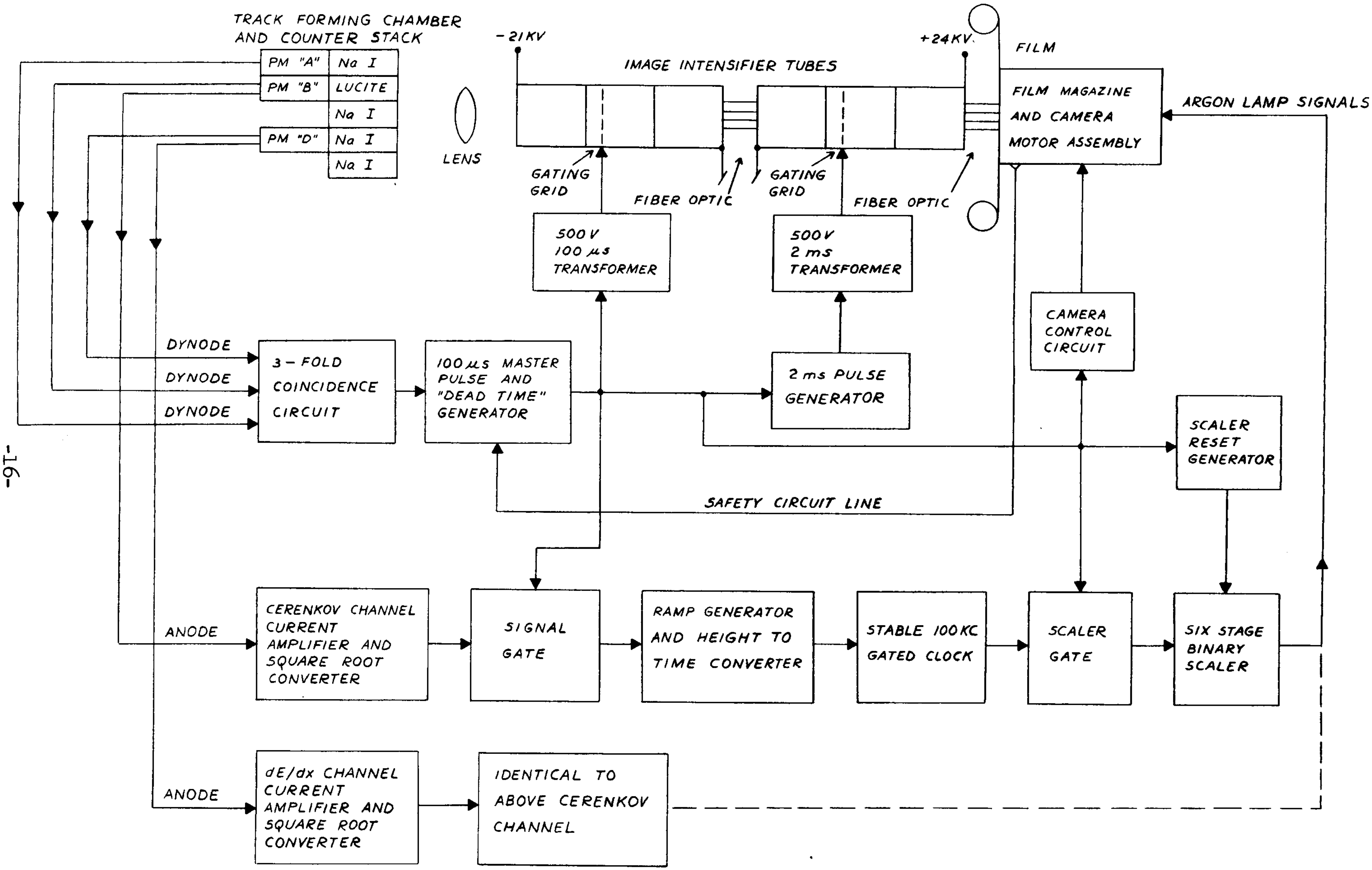


Figure 7. Block Diagram of Complete Luminescent Chamber Experiment

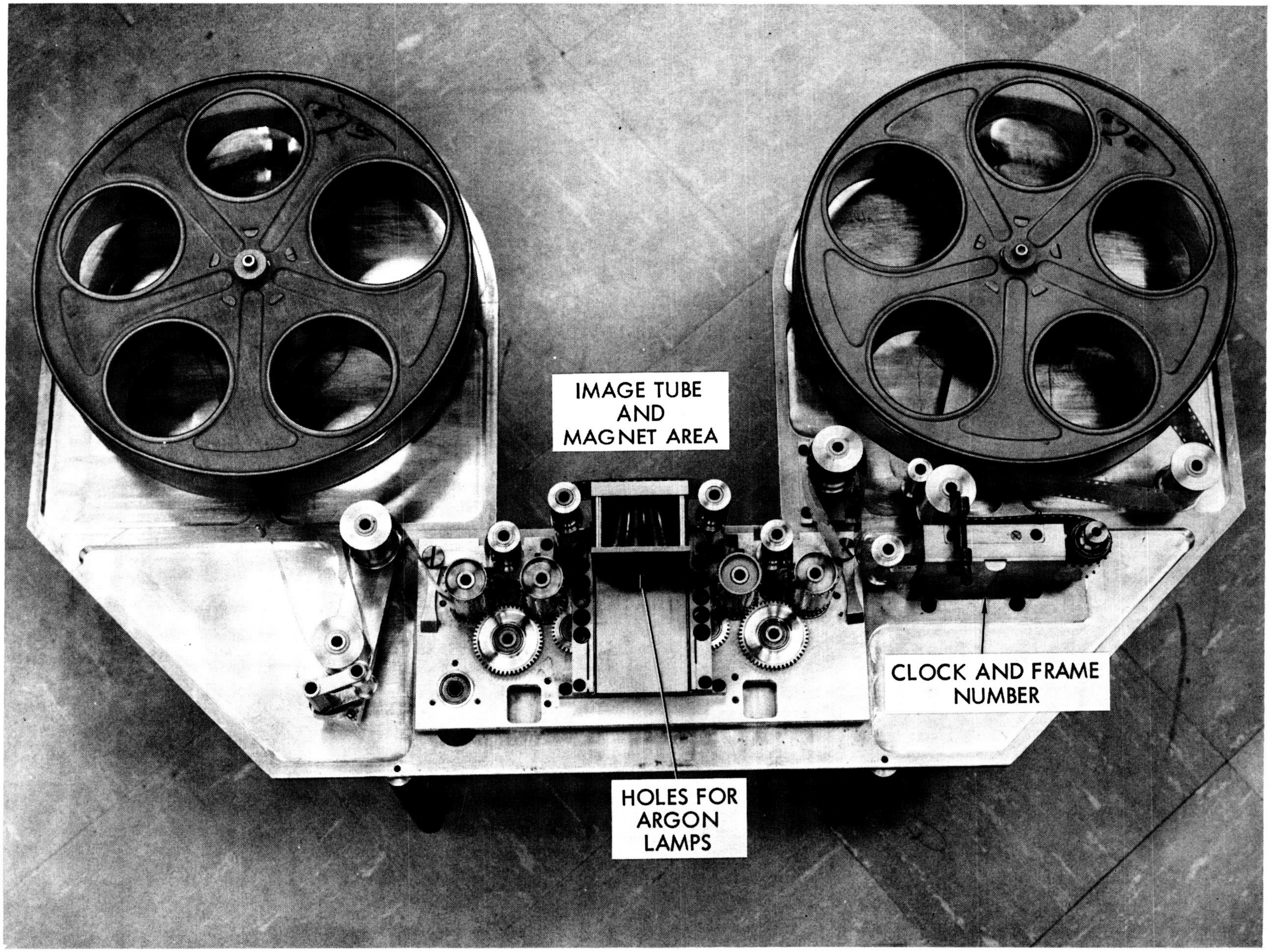


Figure 8. Film Camera with Housing Removed

takes over for the remainder of the cycle. A Geneva movement action accurately meters a one inch advance of the film per event. Dynamic electrical braking is applied to the camera motor at the completion of the cycle to prevent recycling in case of inertial overshoot.

Another microswitch is actuated when the film is exhausted and may be used to signal the release of the balloon and initiate the payload recovery sequence. The film magazine is mated to the image tubes and magnet by a dovetail assembly and sliding shutter so that it can easily be removed from the rest of the system without exposing the film. The entire camera assembly was subcontracted for fabrication to Mardelle Industrial Products of Monrovia, California.

6a. Electronics Design for Image Intensifier Tube Gating and Camera Control

The image intensifier tubes are designed to be cut "off" by applying to the gating grids a negative D.C. bias of several hundred volts with respect to the second stage cathodes. This D. C. potential is supplied through a 10 (20) megohm resistor. The appropriate "on" and "in focus" voltage requires that the grids be several hundred volts positive with respect to the second stage cathodes. Thus, ideally, a square positive pulse of about 500 volts must be developed across the 10 (20) megohm resistor in order to bring the tubes from a cut-off condition to an operating condition.

There were several parameters that had to be determined experimentally in order to choose the optimum rise times and pulse lengths. First, it is important to gate the first tube on in a time short compared to the decay time of the first stage phosphor. It is here that the image is stored following an event in the chamber. Second, the pulse length must be chosen so as to maximize the signal-to-noise ratio. Random noise is generated within the tubes from thermal electrons, field emission, etc. This background, to first order, varies linearly with time.

Therefore, the first tube must be kept on for a time sufficient to receive most of the track information from the first phosphor but not so long that the noise background begins to mask the signal. The main reasons for also gating the second tube are to prevent fogging of the film between events and again to improve the signal-to-noise ratio for any given event. Because of the integrating effect of the phosphors preceding the second stage of the second tube, the rise time of this pulse need not be as fast but the pulse length must be longer. The optimum pulse shapes were determined by measuring the phosphor characteristics as a function of time. This was done using a light pulser at the first image tube cathode to simulate the NaI chamber signal, and a photomultiplier tube at the second tube output phosphor to observe the integrated light output pulses. The results of these measurements indicated that the pulse applied to the grid of the first tube should have a rise time of about 1 microsecond and a width of about 100 microseconds. The pulse for the second tube could have a rise time of about 30 microseconds and should have a width of about 2 milliseconds. The pulse lengths are generated by appropriate univibrators which drive 50 volt transistors. The 50 volt pulses are then applied to pulse transformers with a 10:1 step-up ratio to obtain the required 500 volt pulses. The complete image intensifier tube high voltage supply divider and pulsing electronics is shown in Figs. 9 and 10.

It should be noted that two pulse transformers are necessary to generate the correct pulse shape for the first tube. These were designed and wound in our laboratory on ferrite cores. The first transformer (T1) produces a rise time at the secondary of less than one microsecond and saturates at about 10 microseconds. The pulse at the secondary of the second transformer rises in about 5 microseconds and saturates at about 200 microseconds. By connecting the secondaries of the pulse transformers in parallel through steering diodes 1N547, the required output pulse

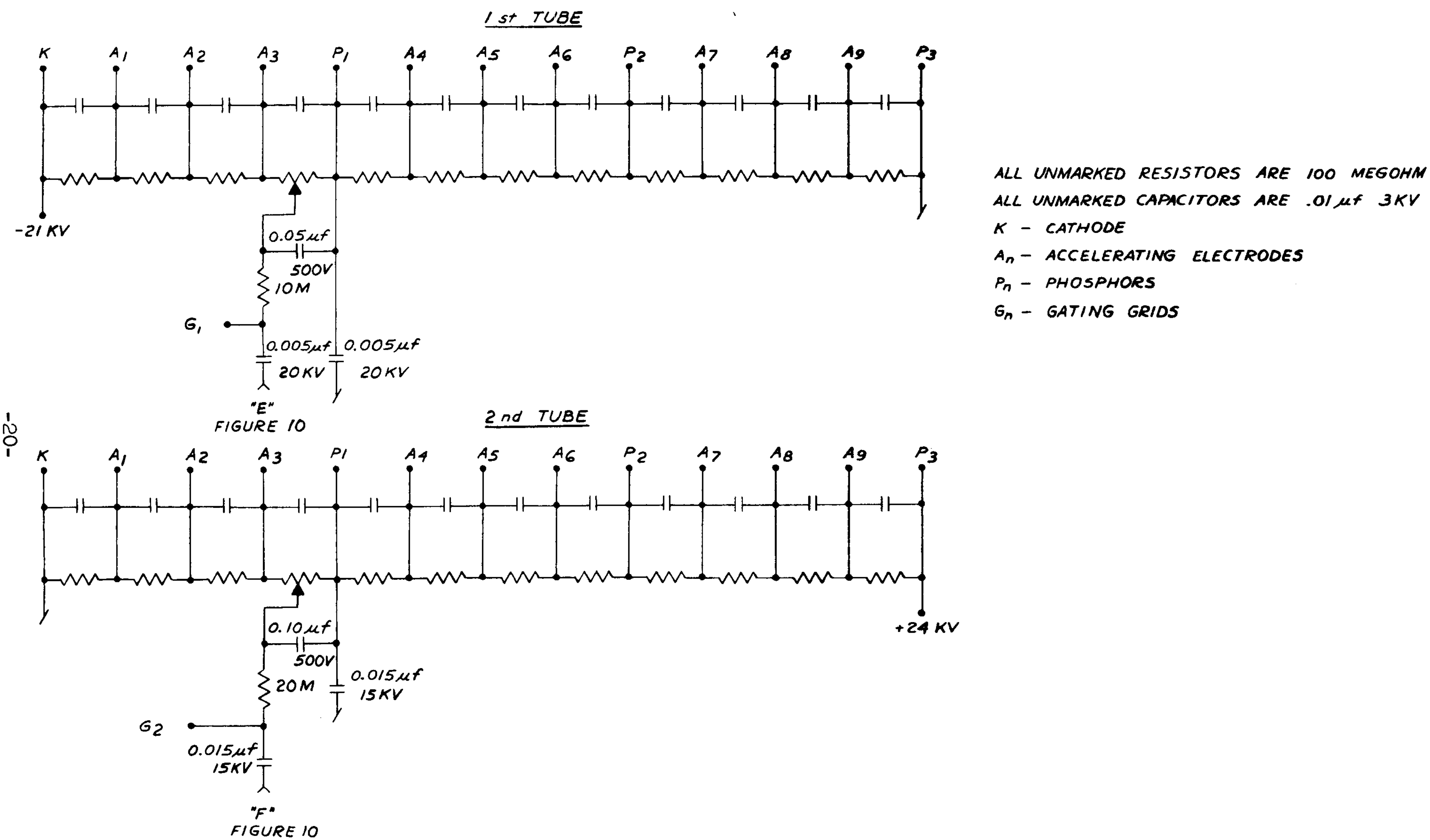


Figure 9. High Voltage Divider Showing Image Intensifier Tube Connections

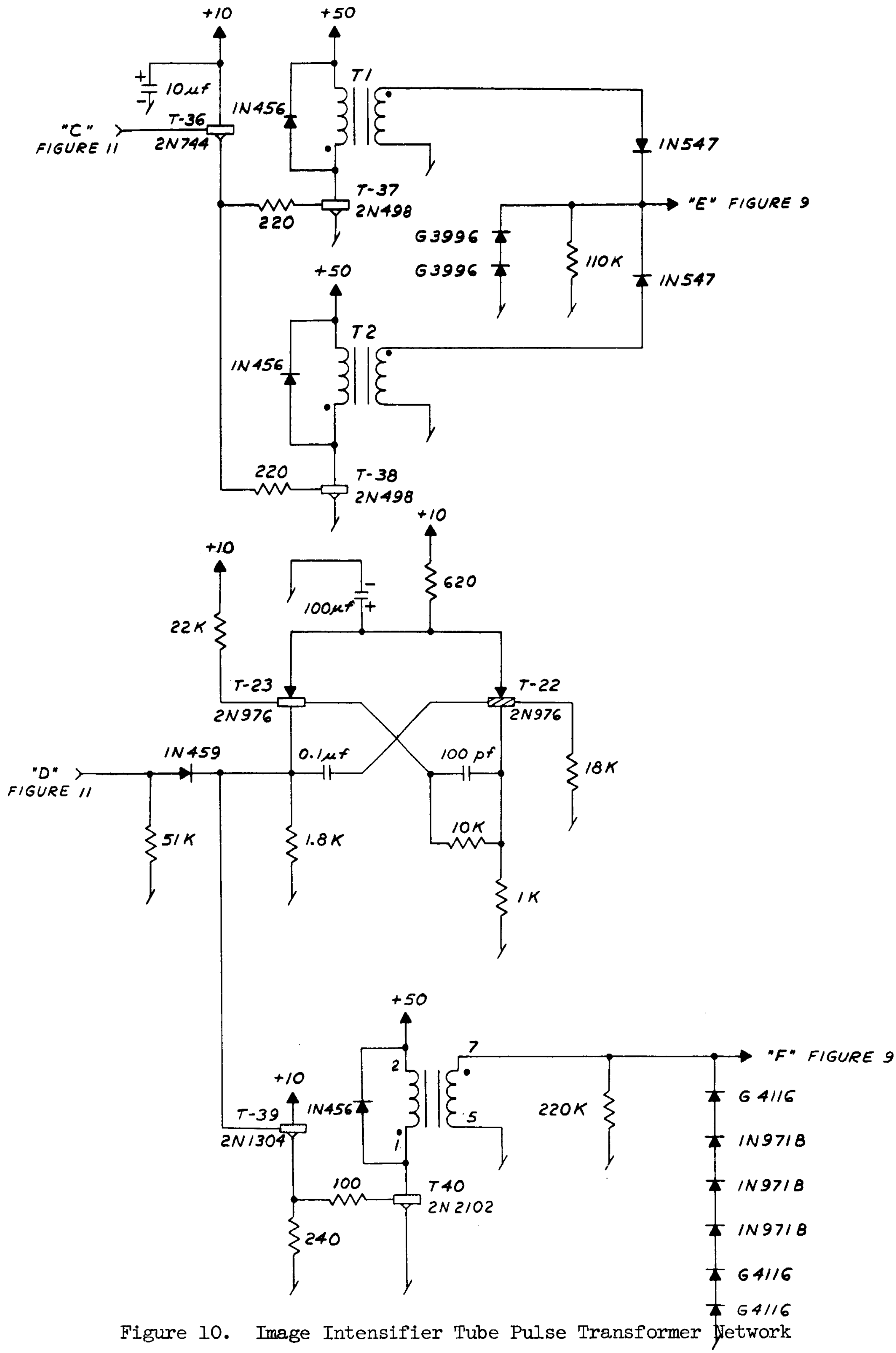


Figure 10. Image Intensifier Tube Pulse Transformer Network

shape is generated. A flat topped pulse is obtained by overdriving the primaries and clipping the secondary pulse height with zener diodes of the required voltage.

The 2 millisecond pulse width and 30 microsecond rise time required for the second tube is generated in a similar fashion. Here, however, a commercial power transformer (UTC H-198) is used as the pulse transformer.

The operation of the electronics which control the camera and image tube gating is described below. Referring to Fig. 11, a negative pulse is applied to the base of T-16. This transistor along with T-17 generates a fast rising master pulse of 100 microseconds duration. The positive pulse from the collector of T-17 is allowed to procede through T-18 only if T-19 is conducting. At the end of the 100 microsecond interval T-20 and T-21 generate a positive pulse which is applied to the base of T-19 and turns this transistor off. It is kept off so that no signal appears at emitter follower T-35 for a time determined by C and other circuit parameters. This "dead time" is built in so that there is sufficient time for the pulse height analysis and the film advance. A safety feature is provided by routing the 15 volt positive signal from the camera motor to point "A" which keeps T-19 turned off for the duration of the camera wind. The pulse at "C" is fed directly to emitter follower T-36, shown on Fig. 10, which in turn drives the high voltage transistor T-37 and pulse transformers for the first image tube. The pulse at "D" is fed to univibrator T-22 and T-23 which generates the 2 millisecond pulse for the second image tube. Points "E" and "F" drive the grids of the respective image intensifier tubes as shown in Fig. 9. Point "B" is fed to the collector of T-41 as shown on the camera control circuit diagram, Fig. 12. T-41 and T-42 generate a 30 millisecond pulse which turns on T-45 and lights argon lamps A1 and A2. These lamps supply the illumination for the clock and message register whose image then appears on the film. At the end of the 30 millisecond interval

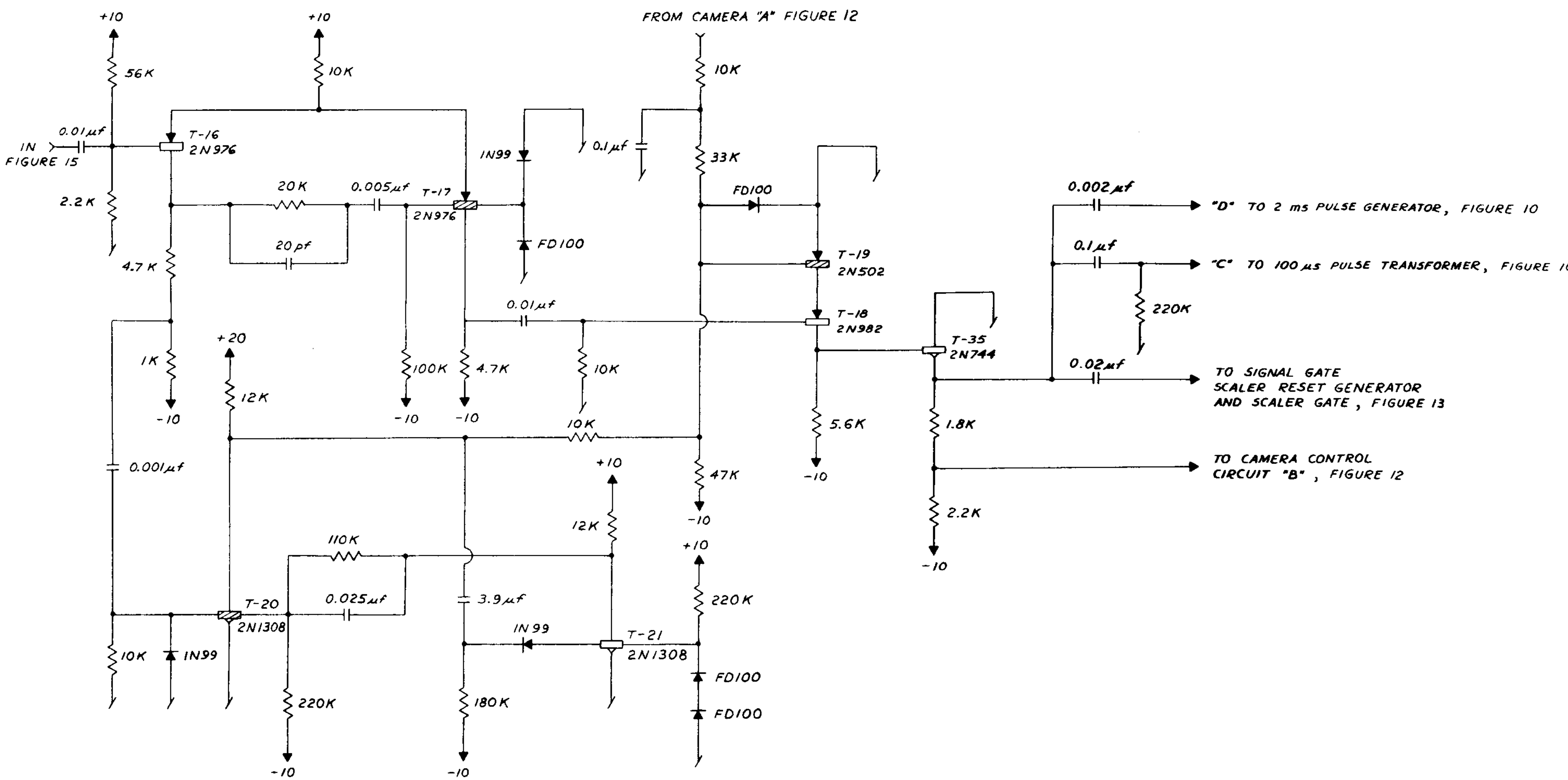


Figure 11. Master Pulse and "Dead Time" Generator

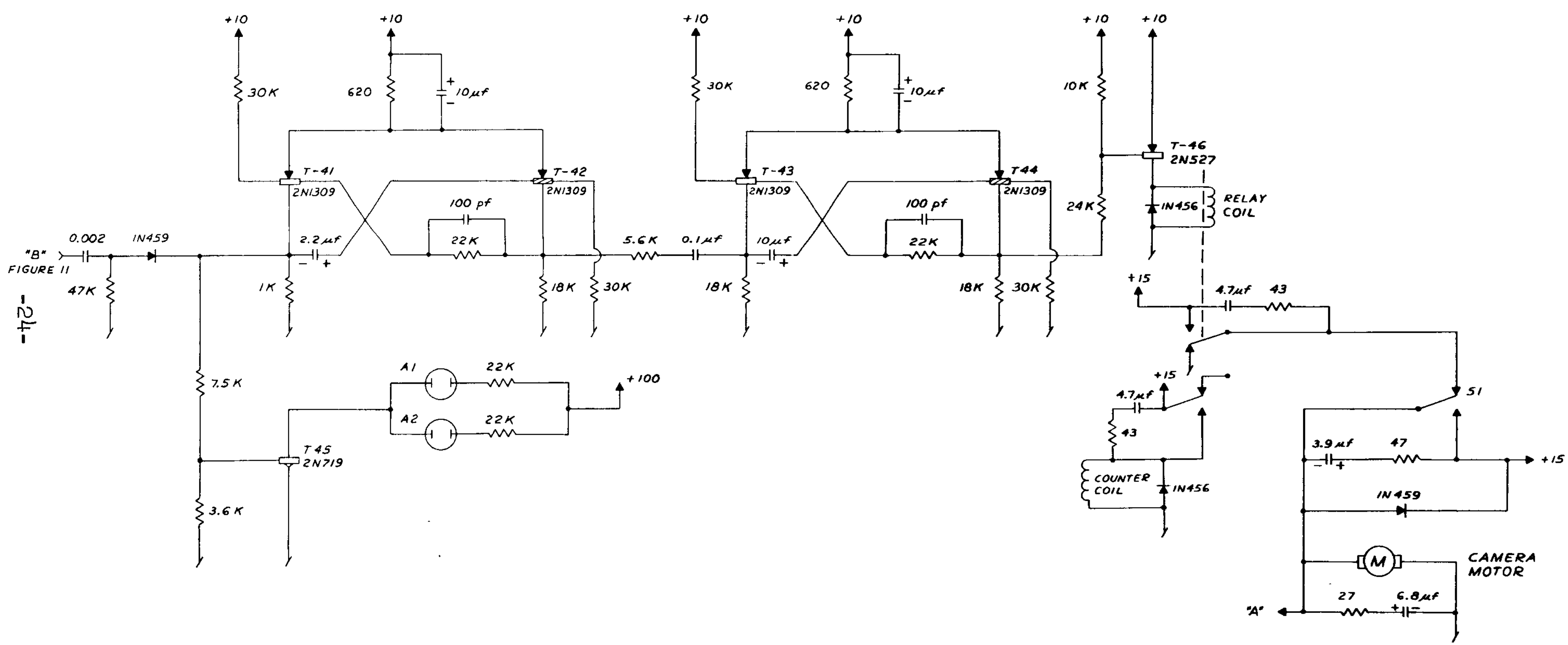


Figure 12. Camera Control Circuit

univibrator T-43 and T-44 applies a pulse to T-46 which closes a relay. One pair of relay contacts supplies D.C power to the camera motor while another pair enables a pulse to be applied to the message register, advancing it one unit. The time constant of T-43, T-44 is chosen to be greater than that time required for the cam operated microswitch, S1, to be actuated but less than the camera wind cycle. When S1 opens and removes power from the camera motor, both poles of the motor are simultaneously grounded which quickly brings the motor to a complete stop. It should be emphasized that the film advance is accurately controlled by the Geneva movement action and not by the time during which the camera motor armature is turning.

6.b. Electronics Design for Pulse Height Analysis

As outlined in Section 3, the pulse height from a Cerenkov radiator and energy loss scintillator is recorded for each event. Since the electronics is nearly identical for both counters, only the Cerenkov channel will be described. The pulse height from the Cerenkov counter is a monotonically increasing function of the particle velocity from the Cerenkov threshold velocity (determined by the index of refraction) up to extreme relativistic velocities. It also varies directly with the square of the charge. This means that for the primary particles ($Z$ = 2 through 8) and velocities, to be investigated in this experiment, the pulse heights to be expected will have a dynamical range of about 160 to 1. In order to keep the electronics as simple as possible and still maintain a linear response in the analyzer over this range, it was decided to introduce a nonlinear amplification of the pulses to compress the range before the actual analysis. Since the statistical fluctuation in the pulse height for any given event is expected to be Poissonian, a standard deviation of plus or minus the square root of the average pulse height must be assigned to each event. For this reason a circuit was designed which would generate an output pulse proportional to the square root of the Cerenkov counter input pulse. In this way the dynamical range is compressed and in addition, each channel of the 64 channel pulse height analyzer will present information of equal statistical weight. The following description refers to Fig. 13. The square root response is approximated, after current amplification, by four appropriately loaded and biased diodes at the base of T-4. A zero D.C. level is maintained at this point by D.C. feedback amplifier T-33 and T-34. The pulse then proceeds through emitter follower T-5 to a signal gate. This gate is opened through T-27 by the master pulse from T-35 in Fig. 11. The gate can be accurately balanced so that no pedestal appears on the output signal which then is stretched by T-6. The following circuit performs the height to time conversion resulting in a pulse across tunnel diode D-1 at the collector of T-10 whose length is proportional to the incoming pulse height. This pulse starts a frequency stabilized 100 kilocycle clock, comprised of multivibrator T-13 and T-14, which runs for the duration of the input pulse length. Before the clock pulses can proceed to the six binary scaler stages shown in Fig. 14, transistor T-15 must be turned on by the scaler gate T-24 and T-25. This gate is also opened by the master pulse from T-35. The scaler gate serves a two-fold purpose. First, the pulse length can be accurately set so that a maximum of 64 cycles of the clock are counted by the scalers. This is to prevent a large pulse that might correspond to say, channel 65, from being counted further by the scalers and registering in channel 1. Thus all pulses whose heights correspond to channel 64 or larger are recorded in channel 64. Second, it also prevents large pulses from the counters, which could override the signal gate in the absence of a master pulse, from actuating the scalers.

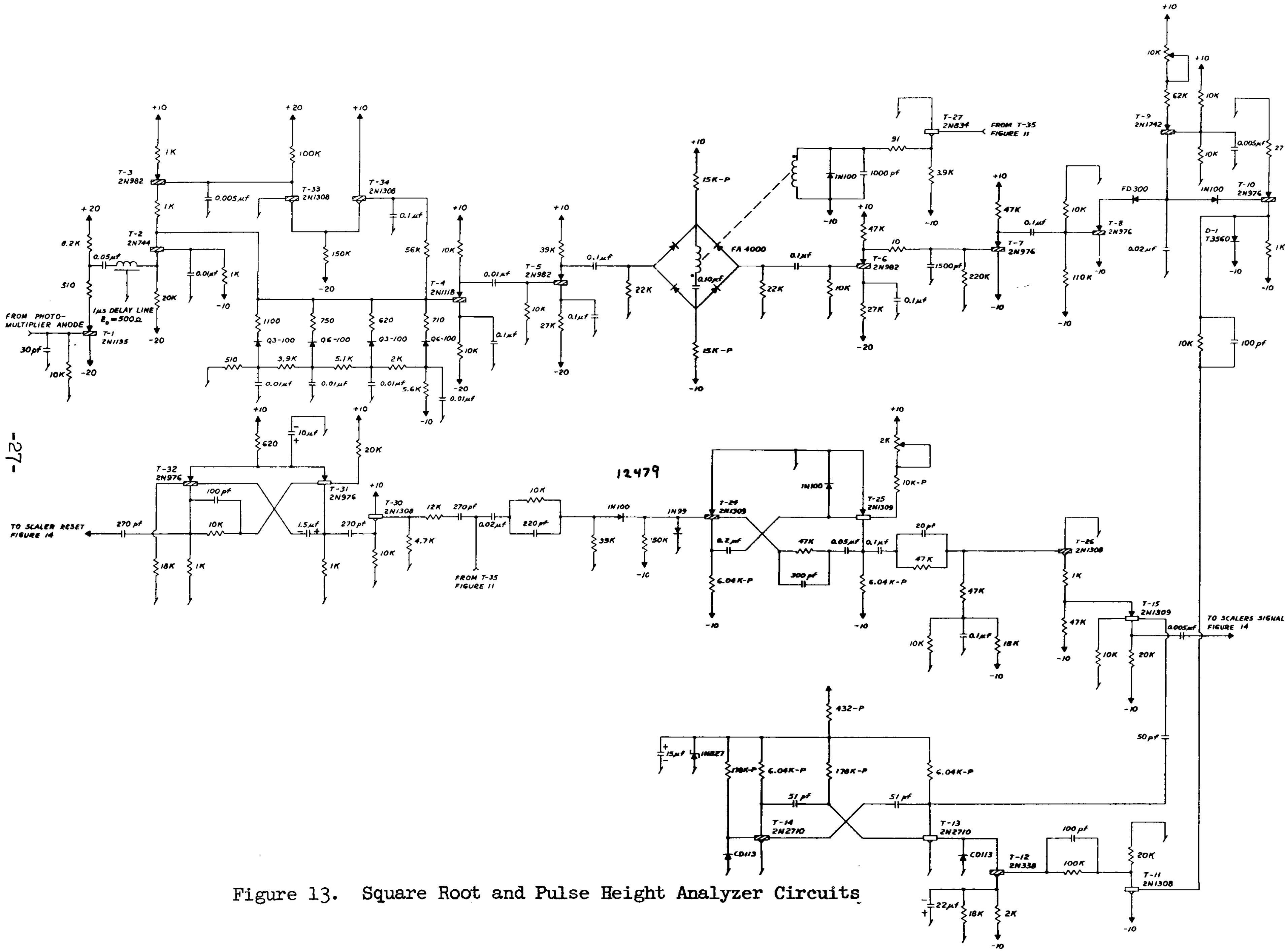


Figure 13. Square Root and Pulse Height Analyzer Circuits

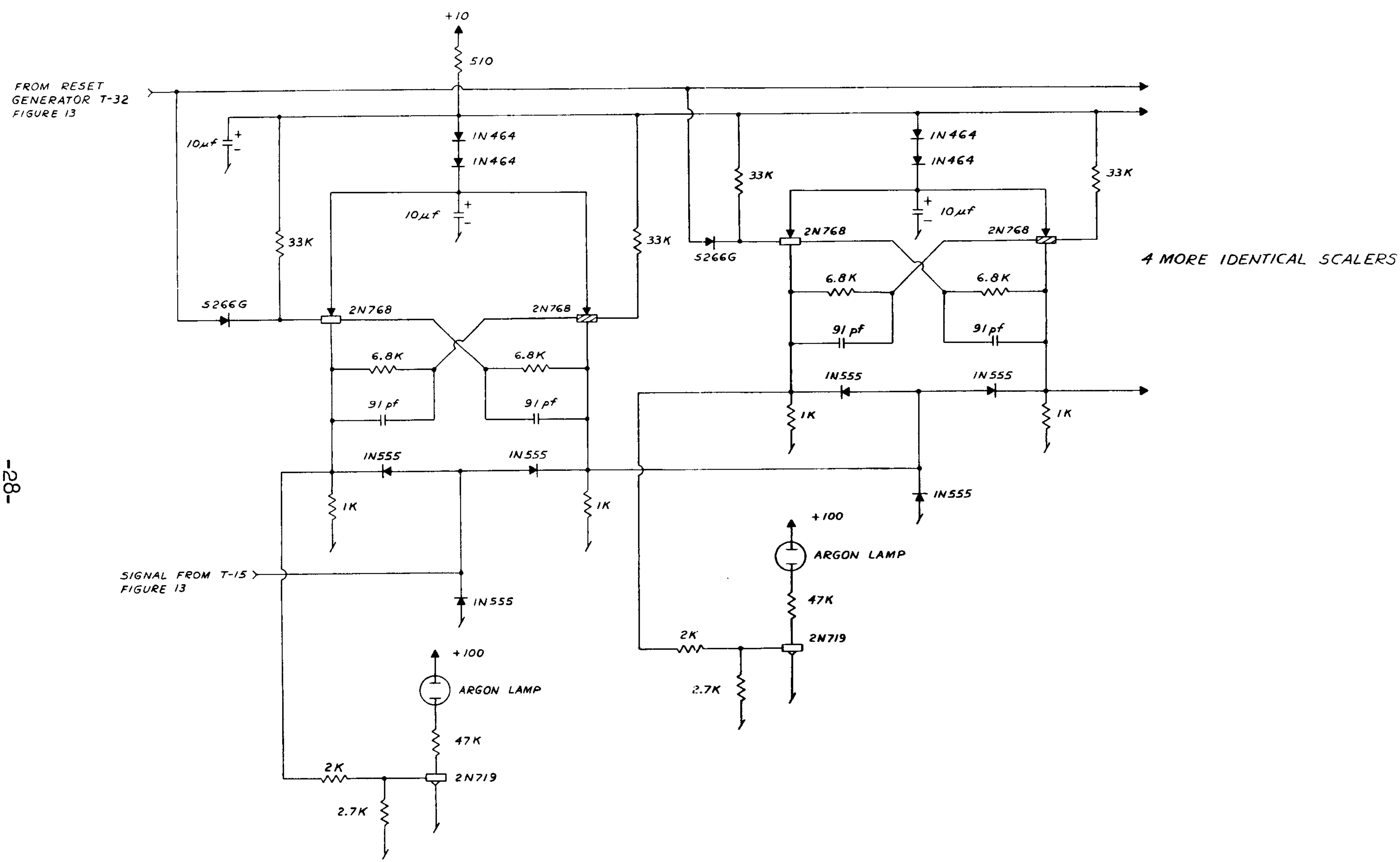


Figure 14. Binary Scaler Circuit

The final state of the scalers is then displayed on the appropriate argon lamps for a time determined by the reset generator T-31 and T-32. The reset generator is also triggered through T-30 by the master pulse from T-35. The output of the reset generator is differentiated and the positive pulse at the end of this predetermined time resets the scalers to their intial state with all lamps off.

The coincidence circuit, whose output triggers the master pulse generator at the base of T-16, is shown in Fig. 15. The emitter followers T-47, T-49 and T-52 are built directly into the bases of the respective photomultiplier tubes. The emitter signals are fed out through shielded cables as shown. D-3 is a one milliampere tunnel diode which is biased in such a way that it does not change its state unless a signal appears simultaneously at all three collectors of limiters T-48, T-51 and T-54. The channel for counter A is straightforward. The channel for counter B (Cerenkov counter) includes a stage of amplification (T-50) since it is desirable to trigger on and investigate particles whose velocity is close to the Cerenkov threshold. The third channel, which looks at the dynode pulses from the NaI (dE/dx) counter D, requires further explanation. Since the primary proton spectrum is not to be investigated in this experiment, a bias must be established in the coincidence circuit which prevents triggering on singly charged particles. This is accomplished by tunnel diode D-2 whose bias is set by proper adjustment of the current in T-53.

The amount of film to be carried during the experiment is limited to 1000 feet, so that the number of events that can be recorded is also limited. From a knowledge of the expected fluxes of the primary nuclei, it is clear that most of the events so recorded would be $\alpha$-particles. In order to obtain better statistics on the higher Z particles, it was decided to incorporate a method of

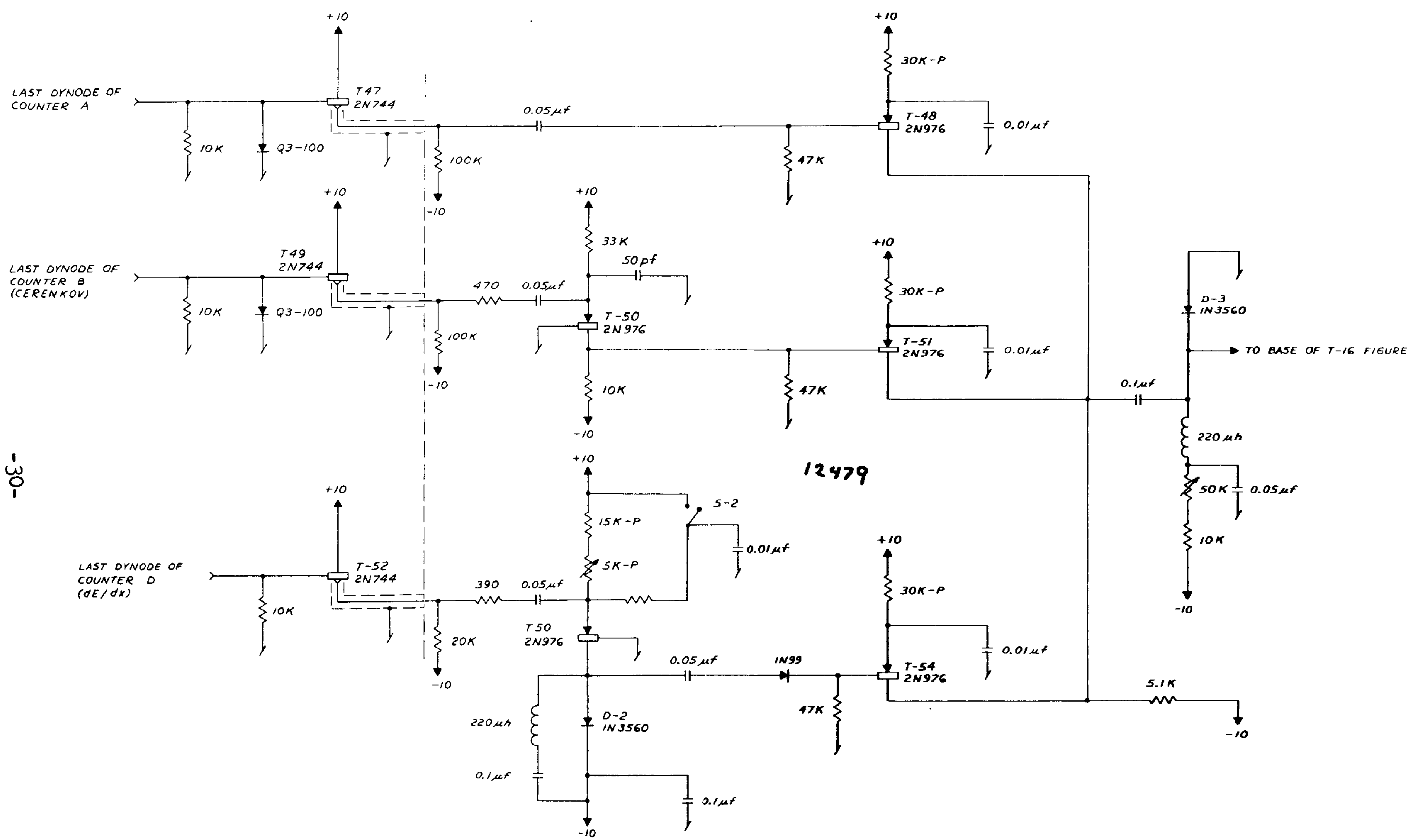


Figure 15. Coincidence Circuit with Threshold Descriminator

changing the bias in flight so as to prevent the recording of $\alpha$-particles after the first few hours. This will be accomplished by an external command which closes relay switch S-2 and changes the bias on D-2.

The entire electronic circuitry, for both channels of pulse height analysis and the image tube, camera, and argon lamp triggering, is built on a total of eleven 3-1/8" x 6-3/4" epoxy circuit boards. Each board has a pair of plug in connectors for signal and power distribution and all boards when mounted and plugged in occupy an electronic package measuring 3-1/2" x 7-1/2" x 10". All the electronics is designed to operate from standard voltages of +10, -10, +20, and -20 volts to be supplied by carbon-zinc batteries and each board contains its own RC filter network for each voltage. In order to conserve power regulated voltages are supplied only to those parts of the circuit that require well regulated voltages, and separate power connections are brought to each board when required for this purpose.

## 7. Mechanical Design and Fabrication

The overall mechanical design, fabrication, and assembly of the various components of the system was carried out in our laboratories. Fig. 16 is a photograph of the completed mechanical system. The "front end" assembly is bolted to the dovetail plate at the opposite end of the magnet by means of the four rods as shown. The track forming and counter stack as well as the lens is mounted on this assembly. The Nikkor f/1.1 lens is positioned so that the 3" x 3" front face of the crystal stack is demagnified by a factor of 3.4 and focused onto the 1-1/2" diameter photocathode of the first image intensifier tube. Provisions were made to enable both the lens and crystal stack to be independently moved parallel to the axis of the system in order to achieve the best optical focus.

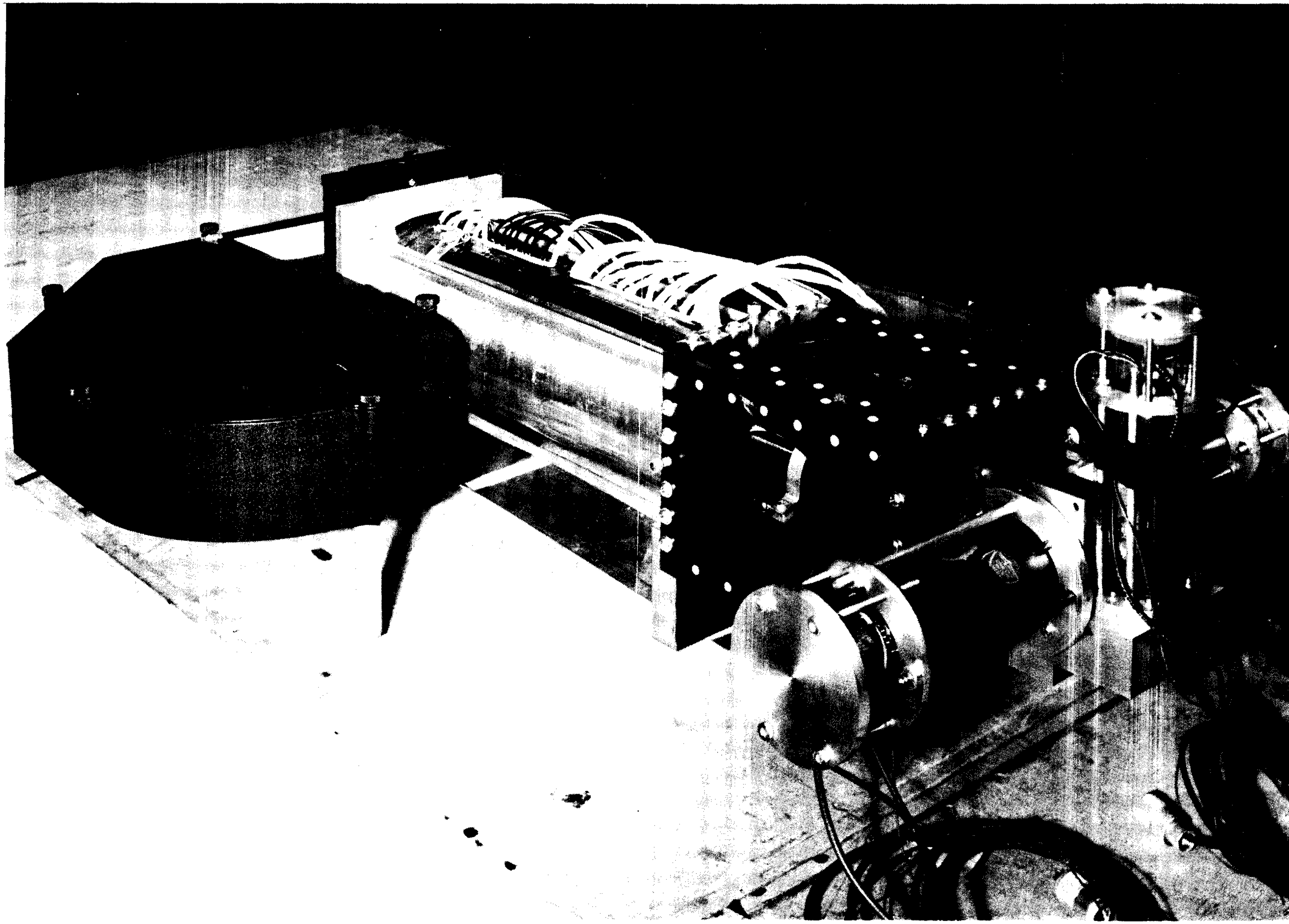

Figure 16. Photograph of Entire Mechanical System

Each of the photomultiplier tubes is located within a cylindrical netic co-netic magnetic shield. The shields are rigidly bolted to the crystal stack assembly. The front windows of the photomultiplier tubes are held in optical contact with their respective light pipes by means of beryllium-copper wave washers mounted under an end cap at the tube bases. Compression is then applied between the end cap and the magnetic shield mount.

The image intensifier tubes are kept under constant longitudinal compression between the end plates of the magnet by a large coil spring mounted inside the magnet. The magnet itself is made up of two semicylindrical sections. These are clamped together by two circular bands which are in turn attached to the two base supports for the entire system. The film magazine is cantilevered from the dovetail plate to assure positive mating at the dovetail interface.

## 8. Final Testing of the Completed Instrument

Before the image tubes were received, the other components of the system were thoroughly tested and adjusted. The pulse height lamps were installed in the camera and the appropriate electronic adjustments were made to obtain the optimum exposure time for both the pulse height lamps and the lamps associated with the clock and message register image. The counter system was determined to be operational by triggering the system from three-fold coincidences initiated by sea level cosmic rays and obtaining the pulse height display on film in exactly the same way as would be done in practice. The observed spectrum and counting rate was in agreement with the calculated cosmic ray mu-meson spectrum and known sea level flux.

The final assembly of the image tube and magnet system was tested in the following way. It was not practical to use the same chamber designed for the multicharged particle experiment in observing tracks due to sea level cosmic rays. The dimensions of the track forming segments are such that only a few track dots per segment result from the passage of a singly charged minimum ionizing particle through the stack. Most of the high energy sea level cosmic rays are of course minimum ionizing singly charged mu-mesons. The minimum charge on particles to be investigated in the course of the experiment is $Z = 2$ resulting in four times as many dots as for $Z = 1$. Therefore, to obtain track pictures and test the operation of the image tubes and gating circuitry, an external NaI chamber was used. This chamber measured 2" x 2" x 4" and was sealed entirely in glass. A 2" x 2" end was demagnified 2:1 and focussed onto the photocathode of the first image intensifier tube. External plastic scintillation counters measuring 2" x 2" were placed above and below the chamber. Cosmic ray two-fold coincidences triggered the system and some of the tracks thus obtained are presented in Fig. 17.

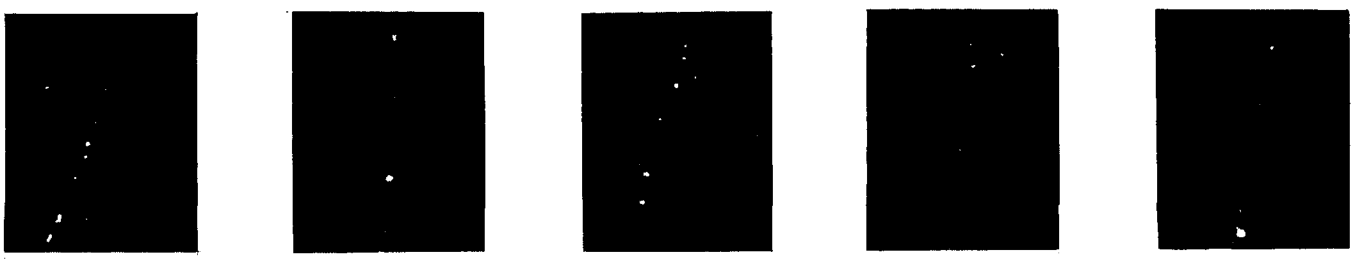

Figure 17. Sea Level Mu-Meson Tracks